Title

Terephthalate Probe for Hydroxyl Radicals: Yield of 2-Hydroxyterephthalic Acid and Transition Metal Interference

Journal

Analytical Letters, 51(15)

ISSN

0003-2719

Authors

Gonzalez, David H
Kuang, Xiaobi M
Scott, John A
et al.

Publication Date

2018-10-13

DOI

10.1080/00032719.2018.1431246

Peer reviewed

The Terephthalate Probe for Hydroxyl Radicals: Yield of 2-Hydroxy Terephthalic acid and Transition Metal Interference

David H. Gonzalez[1], Xiaobi M. Kuang[1], John A. Scott[1,2], Gisele Olimpio de la Rocha[1,3], and Suzanne E. Paulson[1*]

[1]Department of Atmospheric and Oceanic Sciences, University of California, Los Angeles

[2]Department of Chemistry and Biochemistry, University of California, Los Angeles

[3]Instituto de Química, Universidade Federal de Bahia, Bahia, Brazil

Abstract

Hydroxyl radicals (·OH) are key players in chemistry in surface waters, clouds and aerosols. Additionally, ·OH may contribute to the inflammation underlying adverse health outcomes associated with particulate matter exposure. Terephthalate is a particularly sensitive probe for hydroxyl radicals, with a detection limit as low as 2 nM. However, there is uncertainty in ·OH quantification using this method, and potential for interference from fluorescent compounds and from some transition metals. Terephthalate reacts with ·OH to form a fluorescent product, 2-hydroxylterephthalic acid (hTA), with a moderate dependence on pH and temperature. However, there

is disagreement in the literature on the yield of the fluorescent product (Y_{hTA}), which introduces a large uncertainty in the quantification of OH. Additionally, TA and similar organic probes are known to complex Cu(II) at high concentrations, thus if this reaction is important at lower concentrations, Cu(II) could reduce apparent hTA formation, and reduce activity of Cu(II) in target samples. Using a pH 3.5 dark ferrous Fenton system to generate ·OH radicals, we find that Y_{hTA} = 31.5 ± 7%. This is about double the recent literature value measured, but in excellent agreement with earlier measurements. Additionally, we find that interactions between Cu(II) and hTA are small enough to be ignored at Cu(II) concentrations below ~50 μM.

Introduction

·OH plays an important role in various atmospheric and surface water processes. Aerosol aging by ·OH can modify chemical composition (Shrivastava et al. 2008) cloud condensation nuclei (CCN) activity (Shilling et al. 2007) hygroscopic properties (Suda et al. 2014), and optical properties of aerosols (Kim and Paulson 2013). Hydroxyl radical also plays an important role in the chemistry of surface waters (Lindsey and Tarr 2000, Goldstone et al. 2002) degradation of drugs after release into the environment (Rosenfeldt and Linden 2004) in oxidative stress in marine organisms (Lesser 2006) and in waste water treatment (Fernandez-Castro et al. 2015). Inhalation of fine particulate matter has shown correlation with adverse health impacts, including asthma, cardiovascular diseases, pulmonary inflammation, lung cancer and mortality (Brook et al. 2010, Beelen et al.). While the

mechanism(s) by which ambient particles impact health is not yet completely understood, a hypothesized cause under active investigation is oxidative stress, mediated by reactive oxygen species (ROS) (Bates et al. 2015).

A direct measurement of hydroxyl radical in aqueous solutions is difficult due to its low concentrations, short lifetime and chemical and physical similarity to the aqueous solvent. Chemical probes such as benzene (Faust and Allen 1993), nitrobenzene (Zepp et al. 1992), benzoate (Jung et al. 2006), and terephthalate (TA) (Matthews 1980, Fang et al. 1996, Saran and Summer 1999, Snyrychova et al. 2007, Page et al. 2010, Charbouillot et al. 2011) have been used to quantify OH. These methods depend on fluorescence (2-hydroxyterephthalic acid) or UV absorption (benzene derivatives) of oxidation products. Additional approaches such as electron paramagnetic resonance are also available (Shi et al. 2003).

Of the hydroxyl radical probes, terephthalate has several advantages. Due to its symmetric configuration, the ·OH reaction with terephthalate results in only one ring- preserving product, 2-hydroxyterephthalic acid (hTA, Fig. 1). Furthermore, 2-hydroxyterephthalic acid is strongly fluorescent (Armstrong et al. 1963) facilitating detection limits as low as ~2 nM (SI Tab. S1), compared to 30 nM for benzoate (Shen and Anastasio 2012). Further, TA is more soluble, has a more stable fluorescent product and is less susceptible to pH changes compared to several other ·OH probes (Son et al. 2015).

Accurate quantification of ·OH with the terephthalate probe requires knowledge of the yield of the fluorescent product, hTA, per molecule of ·OH reacted. A handful of prior studies have quantified the ·OH formation yield, each with a different source of hydroxyl radicals: Matthews (1980) used radiolysis; Charbouillot et al. (2011) used photolysis of nitrate and H_2O_2 (Fig. 1), Page et al. (2010) used photolysis of nitrite and Mark et al. (1998) used sonication of water. Page et al. (2010) and Mark et al. (1998) but did not show data or indicate a pH for their measurements. The Matthews (1980) (30.5 – 35% increasing as pH increased from 2 - 9), Mark et al. (1998) and Page et al. (2010) (both 35% at unspecified pH) measurements are nearly double those of Charbouillot et al. (2011) (14 – 23% increasing as pH increased from 4 – 7.5). As both the high (Son et al. 2015, An et al. 2016, Batista et al. 2016, Gonzalez et al. 2017) and low (Huang et al. 2013, Paušová et al. 2015, Li et al. 2016, Tafer et al. 2016) values have been taken up in the literature, we attempt to address the discrepancy.

The hTA yield has also been found to depend on O_2 concentration in the sample (Matthews 1980; Saran and Summer 1999); all yields discussed here are for aqueous solutions in equilibrium with air at one atmosphere. Charbouillot et al. (2011) found that the hTA yield is not influenced by ionic strength, ammonium or sulfate ions within the 0.25 – 2 mM range studied, but that the yield has a fairly strong temperature dependence; the yield increases by about a factor of 2 between 278 and 303 K at pH 5.4.

The discrepancy between the measurements of Matthews (1980), Page et al., (2010) and Charbouillot et al. (2011) were suggested by Page et al. (2012) suggested to be due to the photolysis light source used by Charbouillot et al. (2011) also photolyzing hTA, reducing its apparent yield.

While previously unrecognized by the community using TA as a probe for hydroxyl radicals, formation of metal-terephthalate complexes at high concentrations are well known, including with Cu(II), Co(II), Fe(II), Mn(II) and Ni(II) (Acheson and Galwey 1967, Sherif 1970, Rabu et al. 2001, Carson et al. 2009). This presents the possibility that metal interactions with TA might impact the outcome of the assay, either by changing the ability of metals to contribute to chemistry that leads to formation of ·OH or by reducing metal ion availability in solution.

Here, we report a new measurement of the hTA yield, using a different source of OH. Because of the substantial discrepancy between the published datasets, and because there is little data available for the yield of hTA under acidic conditions relevant to water in the atmosphere, such as cloud, fog and rain water (Falconer and Falconer 1980) we measure Y_{hTA} at pH 3.5 using a dark ferrous Fenton system to generate OH. Further, due to its abundance in the atmospheric samples (Wang et al. 2010) here we examine the ability of Cu(II) to interfere with the hTA assay.

Materials and Methods

Materials

Disodium terephthalate (TA) was purchased from TCI America. 2-hydroxy terephthalic acid (hTA) was purchased from Apollo Sci. Methanol (HPLC grade) and sulfuric acid (reagent grade), Chelex® 100 sodium form (50-100 dry mesh), uric acid (>99%), sodium Citrate tribasic dihydrate (>99%), L-ascorbic acid (BioXtra, >99%), L-glutathione reduced (>98%), ethylenediaminetetraacetic acid (EDTA), horseradish peroxidase type II, para-hydroxyphenyl acetic acid, potassium hydrogen phthalate, H_2O_2 (30%) and $FeSO_4$ (>98%) were purchased from Sigma-Aldrich. Sodium phosphate dibasic and potassium phosphate monobasic were purchased from Acros Organics. Ferrozine (4,4'-[3-(2-pyridinyl)-1,2,4-triazine-5,6-diyl] dibenzenesulfonate) was purchased from Fluka Analytic. Hydrophilic Lipophilic Balance cartridges were purchased from Waters (Oasis, 10mg). All materials were used as received.

A rigorous cleaning process was followed for all glass and Teflon containers. After each use, the glass/plastic ware was washed with warm water and soap, then rinsed in deionized (18 MΩ DI) water (3×), ethanol (3×), and finally DI water (3×). The vessels were then soaked in a 1 M nitric acid bath overnight, rinsed with DI water (3x) and air dried. Nitric acid baths were replaced after being used twice.

Stock solutions were prepared with 18 MΩ DI water after further purification by passing through a Chelex column to remove trace metals. pH was measured with a bench top pH meter (HANNA instruments, HI 3220), calibrated daily. Stock solutions of hTA (10^{-3} M) and Fe(II) (5.1 mM) were

wrapped in foil; hTA was kept refrigerated for a few months and Fe(II) was prepared daily and refrigerated. Dissolved oxygen was present in all solutions as solutions were in contact with air and were not degassed.

Fluorescence Spectroscopy and quantification of hTA

hTA fluorescence intensity was measured in single wavelength mode at excitation/emission wavelengths of 310/420 nm with a Lumina Fluorescence Spectrometer (Thermo Scientific). For the purposes of the measurements carried out here, hTA calibration curves were prepared in pH 3.5 or 7.4 solutions at hTA concentrations of 50, 100, 500 and 800 nM. An EEM scan of hTA fluorescence recorded performed with 10 nm excitation and emission slit widths, 5 nm intervals scanning at 60 nm/s with 10 ms integration time (SI Fig. S1). A 10^{-3} M Stock solution of hTA in milli-Q water (18 MΩ) was prepared using an acid cleaned Teflon bottle which was wrapped in aluminum, and stored in the refrigerator. A 5-point calibration was performed prior to each experiment.

Quantification of Fe(II)

Fe(II) was quantified with the ferrozine method (Stookey 1970) using a liquid waveguide capillary cell (LWCC-3100, World Precision Instruments Inc.), a UV-Vis light source (AvaLight-DHS, Avantes) and UV-Vis spectrometer (AvaSpec 2048L, Avantes). The Fe(II)-ferrozine complex has a maximum absorbance at 562 nm (A_{562}). To account for instrument drift and solution turbidity, the absorbance at 700 nm (A_{700}) was subtracted from A_{562}. Aliquots were analyzed by adding 10 µL of 5.1 mM ferrozine to 2.0 mL aliquots. Fe(II)

calibration curves are made by preparing a stock solution of 2 mM Iron Sulfate (Sigma-Aldrich) at pH 3.5 and diluting to between 0.012 and 0.75 µM Fe(II).

Quantification of H_2O_2

Quantification of aqueous H_2O_2 was performed using a High Performance Liquid Chromatograph equipped with a fluorescence detector (Shimadzu RF-10AXL detector) (Arellanes et al. 2006). The eluent, water with 0.1 mM EDTA adjusted to pH 3.5 with 0.1 N sulfuric acid, was delivered at 0.6 mL/min to a C18 guard column. H_2O_2 elutes at 0.5 min, after which it is mixed with a fluorescent reagent containing horseradish peroxidase and para-hydroxyphenyl acetic acid (POHPAA). The peroxidase enzyme catalyzes a reaction between H_2O_2 and POHPAA to form a fluorescent dimer, which is detected at the $\lambda_{ex}/\lambda_{em}$ 320/400nm. The solution is mixed with ammonium hydroxide (30%) to increase its fluorescence intensity prior to detection. The HPLC was calibrated at least weekly with 10^{-8} to 10^{-6} M standards prepared from a 0.3% stock solution, titrated with sodium thiosulfate to determine the concentration.

Oxidation of TA via a Ferrous Fenton System

Experiments to derive hTA yields were carried out as follows. Triplicate samples of 4.44-4.77 µM $FeSO_4$ and 5.38-6.00 µM H_2O_2 (SI Tab. S2) were mixed with excess terephthalate (~500 µM, 100-fold excess) in 60 mL Teflon bottles and allowed to react in the dark with gentle shaking (25 rpm, Heidolph Rotamax) at 20° C. $FeSO_4$ was added last as to initiate the Fenton

reaction. The resulting solution was monitored in triplicate for H_2O_2, Fe(II) and hTA every 20 minutes for 2 h. Initial concentrations of H_2O_2 and Fe(II) are shown in SI Tab. S2. Blanks consisted of TA in pH 3.5. Aliquots were diluted by 5 - 10x to fall within the ranges of detection for Fe(II) and H_2O_2. At µM concentrations, the system is sensitive to trace contaminants, including metals and organics, which can change ·OH formation chemistry and/or the ability of terephthalate to scavenge all available OH, thus rigorous cleaning, dust exclusion and high purity reagents were critical for these experiments.

A 54-reaction chemical kinetics model (SI Tab. S3) including reactions describing Fenton chemistry, acid-base equilibria, iron sulfate chemistry and odd oxygen free radical chemistry was developed to derive hTA yields. Concentrations as a function of time were calculated from initial concentrations using FACSIMILIE (MCPA Software, UK).

Interference of Cu(II) with the hTA assay

EEM scans were performed to probe fluorescence of terephthalate and Cu(II) complex, if any. The potential reduction of hTA fluorescence intensity by Cu(II) was probed by adding 1µM to 250 µM of Cu(II) to 800nM hTA, and measuring fluorescence using the single-wavelength scan mode after 2 hours. Additionally, H_2O_2 formation from 20 µm Cu(II) with different concentrations of TA (0.5 to 10mM) was measured every 30 minutes for 2 hours. 20 µM of Cu(II) was chosen because in aqueous solutions at pH 3.5 this concentration produces significant amounts of H_2O_2 in the dark (this work, SI Fig. S2).

Results

Hydroxyterephthalate Yield

Fig. 1 shows experimental data (symbols) and model best fit (lines) for the average of three experiments; error bars show the standard deviation of nine measurements at each time point (three replicates from each of three experiments). The model is most sensitive to the rate constant for Fe(II) reacting with H_2O_2 to make $^{\cdot}OH$ and co-products (the Fenton reaction, k_{15} in SI Tab. S3). Most published rates for this reaction fall within the range 55 -76 $M^{-1}s^{-1}$ (Zuo and Hoigne 1992, De Laat and Le 2005). The best fit between the model and the measured H_2O_2 and Fe(II) was obtained using 76 $M^{-1}s^{-1}$ for the Fenton reaction. This results in mean square errors (MSEs) of 4.3 and 3.1 % for Fe(II) and H_2O_2, respectively (Fig. 1). We then adjusted the yield of hTA (Y_{hTA}) to minimize the MSE between the model and the average concentration of hTA, and found a best-fit Y_{hTA} = 31.5 ± 7%, with and MSE of 0.24%. Altering Y_{hTA} does not affect the modeled Fe(II) and H_2O_2 concentrations. The error bars for the yield were derived by finding the best fit Y_{hTA} for ± 1 σ of the measured hTA concentrations (Fig. 1). At pHs above 4, formation of iron hydroxide and iron sulfate precipitates increase (De Laat and Le 2005), compromising the utility of the Fe(II)/H_2O_2 system as an $^{\cdot}OH$ source, so we were not able to measure Y_{hTA} at higher pHs.

Fig. 2 summarizes reported measurements of hTA yields as a function of pH. Our results are in excellent agreement with the results of Matthews

(1980) and about double those of Charbouillot et al. (2011). Some of the difference is explained by the temperature dependence reported by Charbouillot et al. (2011) (above). Differences in the temperature of this work (293 K) and Charbouillot et al. (2011) (288 K) would suggest a difference of about 20% (Matthews et al. (1980) did not report a temperature. To generate ·OH radicals, Matthews (1980) used radiolysis, while Charbouillot et al. (2011) photolyzed either nitrate or H_2O_2 using a 1000 W xenon lamp (λ > 300 nm). In a separate study, Page et al. (2010) reported that the UV absorption spectrum for hTA contains a weak absorption between 275 - 365 nm, with a slight pH dependence. Wavelengths below 365 nm were observed to cause some decomposition of hTA, leading the researchers to conclude that nitrate photolysis could not be used to probe hTA formation (Page et al. 2012). Charbouillot et al. (2011) had good agreement between their results using nitrate or H_2O_2 as the ·OH source, but since they used the same lamp, similar degradation of hTA likely occurred. We conclude that the Matthews (1980) yields, together with this work and Page et al. (2010) are correct and recommend a yield of 35% for pHs above 9, decreasing monotonically to 30.5% at pH 2 with the expression Y_{hTA} (%) = 30 + 0.43 × pH, and possibly decreasing more below pH 2.

Potential interference of Cu(II) with hTA assay

We performed several experiments to explore the potential for Cu(II) to interfere with TA of hTA, and vise-versa. At high concentrations, terephthalate and Cu(II) in water at pH3.5 rapidly form a blue precipitate

(Carson et al. 2009). However, mixtures of 1 – 250 µM Cu(II) and 10 mM TA did not produce an observable precipitate (this study), and further did not exhibit fluorescence in EEM scans. Next, we investigated if TA changes Cu(II) reactivity by investigating the effect of added TA on the formation of H_2O_2 from 200 µM Cu(II). The results indicate a decrease in H_2O_2 formation that, while statistically significant at the $p < 0.5$ level (SI Fig. S2s), was very slight; over the TA concentration range of 0.5 to 10 mM, the decrease was less than 2%.

Fig. 3 shows the reduction in fluorescence intensity of 800 nM hTA with added Cu(II) in both pH3.5 and phosphate buffer. The result showed that significant reduction (>10%) of hTA intensity occurs only at concentration above about 50 µM of Cu(II) (Fig. 3), a high concentration relative to copper concentrations in many environmental extracts (e.g., Wang et al. 2010). We conclude that under most conditions, Cu(II) does not interfere with the TA assay, or vis-versa.

Conclusions

The terephthalate method for quantification of hydroxyl radical is a robust, straightforward method under most conditions, and it can often be used with a stand-alone fluorescence spectrometer without the need for prior separation. To calculate the ·OH concentration, the yield of hTA from the ·OH reaction with TA is required; best estimates off this yield are 35% at pH 9 or above, decreasing monotonically to 31% at pH = 2. The potential for direct

interactions between TA and soluble metals such as Cu (II) should be considered if target samples contain high (high μM - mM range) concentrations of metals.

Acknowledgements

This material is based upon work supported by the U.S. National Science Foundation under Grant No. 443956-PA-22671. The views and opinions expressed in this manuscript are those of the authors. We gratefully acknowledge Messrs. Yu Zhong, Zane Karl and Kevin Huynh and Christopher Cala for their valuable assistance in the laboratory.

References

Acheson, R. and A. Galwey (1967). The thermal decomposition of nickel terephthalate and nickel salts of other carboxylic acids. J. Chem. Soc. A: Inorg. Phys. Theor. 1: 1174-1178.

An, J., G. Li, T. An and X. Nie (2016). Indirect photochemical transformations of acyclovir and penciclovir in aquatic environments increase ecological risk. Env. Tox. Chem. **35**(3): 584-592.

Arellanes, C., S. E. Paulson, P. M. Fine and C. Sioutas (2006). Exceeding of Henry's Law by Hydrogen Peroxide Associated with Urban Aerosols. . Envir. Sci. Tech. **40** (16): 4859-4866.

Armstrong, W. A., R. A. Facey, D. W. Grant and W. G. Humphreys (1963). A tissue-equivalent chemical dosimeter sensitive to 1 rad. Can. J. Chem. **41**(6): 1575-1577.

Bates, J. T., R. J. Weber, J. Abrams, V. Verma, T. Fang, M. Klein, . . . A. G. Russell (2015). Reactive Oxygen Species Generation Linked to Sources of Atmospheric Particulate Matter and Cardiorespiratory Effects. Env. Sci. Tech. **49**(22): 13605-13612.

Batista, A. P. S., A. C. S. C. Teixeira, W. J. Cooper and B. A. Cottrell (2016). Correlating the chemical and spectroscopic characteristics of natural organic matter with the photodegradation of sulfamerazine. Water Res. **93**(Supplement C): 20-29.

Beelen, R., O. Raaschou-Nielsen, M. Stafoggia, Z. J. Andersen, G. Weinmayr, B. Hoffmann, . . . G. Hoek (2014). Effects of long-term exposure to air pollution on natural-cause mortality: an analysis of 22 European cohorts within the multicentre ESCAPE project. Lancet **383**(9919): 785-795.

Brook, R. D., S. Rajagopalan, C. A. Pope, J. R. Brook, A. Bhatnagar, A. V. Diez-Roux, . . . J. D. Kaufman (2010). Particulate Matter Air Pollution and Cardiovascular Disease. An Update to the Scientific Statement From the American Heart Association **121**(21): 2331-2378.

Carson, C. G., K. Hardcastle, J. Schwartz, X. Liu, C. Hoffmann, R. A. Gerhardt and R. Tannenbaum (2009). Synthesis and structure characterization of copper terephthalate metal–organic frameworks. Eur. J. Inorg. Chem. **2009**(16): 2338-2343.

Charbouillot, T., M. Brigante, G. Mailhot, P. R. Maddigapu, C. Minero and D. Vione (2011). Performance and selectivity of the terephthalic acid probe for (OH)-O-center dot as a function of temperature, pH and composition of atmospherically relevant aqueous media. J. Photochem. Photobiol. a-Chem. **222**(1): 70-76.

De Laat, J. and T. G. Le (2005). Kinetics and modeling of the Fe (III)/H2O2 system in the presence of sulfate in acidic aqueous solutions. Env. Sci. Tech. **39**(6): 1811-1818.

Falconer, R. and P. Falconer (1980). Determination of cloud water acidity at a mountain observatory in the Adirondack Mountains of New York State. Journal of Geophysical Research: Oceans **85**(C12): 7465-7470.

Fang, X. W., G. Mark and C. vonSonntag (1996). OH radical formation by ultrasound in aqueous solutions .1. The chemistry underlying the terephthalate dosimeter. Ultrasonics Sonochem. **3**(1): 57-63.

Faust, B. C. and J. M. Allen (1993). Aqueous-phase photochemical formation of hydroxyl radical in authentic cloudwaters and fogwaters. Env. Sci. Tech. **27**(6): 1221-1224.

Fernandez-Castro, P., M. Vallejo, M. F. San Roman and I. Ortiz (2015). Insight on the fundamentals of advanced oxidation processes. Role and review of the determination methods of reactive oxygen species. J. Chem. Tech. Biotech. **90**(5): 796-820.

Goldstone, J. V., M. J. Pullin, S. Bertilsson and B. M. Voelker (2002). Reactions of hydroxyl radical with humic substances: Bleaching, mineralization, and production of bioavailable carbon substrates. Env. Sci. Tech. **36**(3): 364-372.

Gonzalez, D. H., C. K. Cala, Q. Y. Peng and S. E. Paulson (2017). HULIS Enhancement of Hydroxyl Radical Formation from Fe(II): Kinetics of Fulvic Acid-Fe(II) Complexes in the Presence of Lung Antioxidants. Env. Sci. Tech. **51**(13): 7676-7685.

Huang, W., M. Brigante, F. Wu, K. Hanna and G. Mailhot (2013). Effect of ethylenediamine-N,N′-disuccinic acid on Fenton and photo-Fenton processes using goethite as an iron source: optimization of parameters for bisphenol A degradation. Envir. Sci. Poll. Res. **20**(1): 39-50.

Jung, H., B. Guo, C. Anastasio and I. M. Kennedy (2006). Quantitative measurements of the generation of hydroxyl radicals by soot particles in a surrogate lung fluid. Atmos. Environ. **40**(6): 1043-1052.

Kim, H. and S. E. Paulson (2013). Real refractive indices and volatility of secondary organic aerosol generated from photooxidation and ozonolysis of limonene, alpha-pinene and toluene. Atmos. Chem. Phys., **13**(15): 7711-7723.

Lesser, M. P. (2006). Oxidative stress in marine environments: Biochemistry and physiological ecology. Annu. Rev. Physiol. Palo Alto, Annual Reviews. **68:** 253-278.

Li, R., C. Zhao, B. Yao, D. Li, S. Yan, K. E. O'Shea and W. Song (2016). Photochemical Transformation of Aminoglycoside Antibiotics in Simulated Natural Waters. Env. Sci. Tech. **50**(6): 2921-2930.

Lindsey, M. E. and M. A. Tarr (2000). Inhibition of hydroxyl radical reaction with aromatics by dissolved natural organic matter. Env. Sci. Tech. **34**(3): 444-449.

Mark, G., A. Tauber, R. Laupert, H.-P. Schuchmann, D. Schulz, A. Mues and C. von Sonntag (1998). OH-radical formation by ultrasound in aqueous solution – Part II: Terephthalate and Fricke dosimetry and the influence of various conditions on the sonolytic yield. Ultrasonics Sonochemistry **5**(2): 41-52.

Matthews, R. W. (1980). The radiation-chemistry of the terephthalate dosimeter. Radiation Res. **83**(1): 27-41.

Page, S. E., W. A. Arnold and K. McNeill (2010). Terephthalate as a probe for photochemically generated hydroxyl radical. J. Environ. Monitor. **12**(9): 1658-1665.

Page, S. E., M. Sander, W. A. Arnold and K. McNeill (2012). Hydroxyl Radical Formation upon Oxidation of Reduced Humic Acids by Oxygen in the Dark. Env. Sci. Tech. **46**(3): 1590-1597.

Paušová, Š., J. Krýsa, J. Jirkovský, C. Forano, G. Mailhot and V. Prevot (2015). Insight into the photocatalytic activity of ZnCr–CO3 LDH and derived mixed oxides. Applied Catalysis B: Environmental **170-171**(Supplement C): 25-33.

Rabu, P., J. Rueff, Z. Huang, S. Angelov, J. Souletie and M. Drillon (2001). Copper (II) and cobalt (II) dicarboxylate-based layered magnets: influence of π electron ligands on the long range magnetic ordering. Polyhedron **20**(11): 1677-1685.

Rosenfeldt, E. J. and K. G. Linden (2004). Degradation of endocrine disrupting chemicals bisphenol A, ethinyl estradiol, and estradiol during UV photolysis and advanced oxidation processes. Env. Sci. Tech. **38**(20): 5476-5483.

Saran, M. and K. H. Summer (1999). Assaying for hydroxyl radicals: Hydroxylated terephthalate is a superior fluorescence marker than hydroxylated benzoate. Free Radical Res. **31**(5): 429-436.

Shen, H. and C. Anastasio (2012). A comparison of hydroxyl radical and hydrogen peroxide generation in ambient particle extracts and laboratory metal solutions. Atmos. Environ. **46**: 665-668.
Sherif, F. G. (1970). Heavy metal terephthalates. Indust. Eng. Chem. Prod. Res. Dev. **9**(3): 408-412.
Shi, T. M., R. P. F. Schins, A. M. Knaapen, T. Kuhlbusch, M. Pitz, J. Heinrich and P. J. A. Borm (2003). Hydroxyl radical generation by electron paramagnetic resonance as a new method to monitor ambient particulate matter composition. J. Env. Monitor. **5**(4): 550-556.
Shilling, J. E., S. M. King, M. Mochida and S. T. Martin (2007). Mass spectral evidence that small changes in composition caused by oxidative aging processes alter aerosol CCN properties. J. Phys. Chem. A **111**(17): 3358-3368.
Shrivastava, M. K., T. E. Lane, N. M. Donahue, S. N. Pandis and A. L. Robinson (2008). Effects of gas particle partitioning and aging of primary emissions on urban and regional organic aerosol concentrations. Journal of Geophysical Research-Atmospheres **113**(D18): 16.
Snyrychova, I., P. Kos and E. Hideg (2007). First application of terephthalate as a fluorescent probe for hydroxyl radicals in thylakoid membranes. Photosynthesis Res. **91**(2-3): 307-307.
Son, Y., V. Mishin, W. Welsh, S.-E. Lu, J. Laskin, H. Kipen and Q. Meng (2015). A Novel High-Throughput Approach to Measure Hydroxyl Radicals Induced by Airborne Particulate Matter. Int. J. Env. Res. Public Health **12**(11): 13678.
Stookey, L. L. (1970). Ferrozine---a new spectrophotometric reagent for iron. Analytical Chemistry **42**(7): 779-781.
Suda, S. R., M. D. Petters, G. K. Yeh, C. Strollo, A. Matsunaga, A. Faulhaber, . . . S. M. Kreidenweis (2014). Influence of Functional Groups on Organic Aerosol Cloud Condensation Nucleus Activity. Env. Sci. Tech. **48**(17): 10182-10190.
Tafer, R., M. Sleiman, A. Boulkamh and C. Richard (2016). Photomineralization of aqueous salicylic acids. Photoproducts characterization and formation of light induced secondary OH precursors (LIS-OH). Water Res. **106**: 496-506.
Wang, Y., C. Arellanes, D. Curtis and S. E. Paulson (2010). Probing the Source of Hydrogen Peroxide Generation by Coarse Mode Aerosols in Southern California. Env. Sci. Tech. **44**: 4070-4075.
Zepp, R. G., B. C. Faust and J. Hoigne (1992). Hydroxyl radical formation in aqueous reactions (pH 3-8) of iron (II) with hydrogen peroxide: the photo-Fenton reaction. Env. Sci. Tech. **26**(2): 313-319.
Zuo, Y. and J. Hoigne (1992). Formation of hydrogen peroxide and depletion of oxalic acid in atmospheric water by photolysis of iron (III)-oxalato complexes. Env. Sci. Tech. **26**(5): 1014-1022.

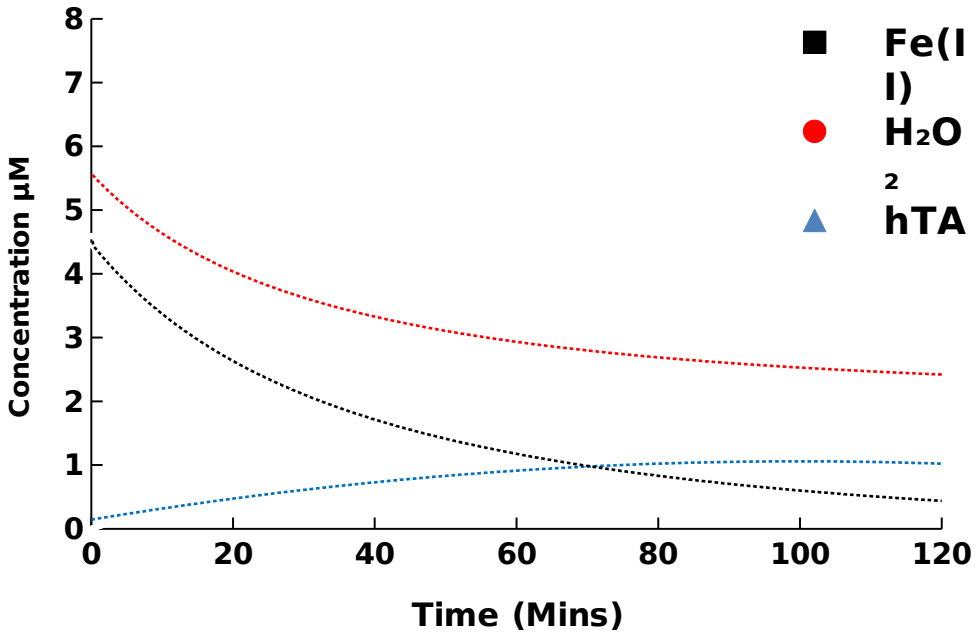

Figure 1. Concentration profiles of Fe(II), H_2O_2 and hTA averaged from triplicate measurements of three experimental trials. Error bars represent ± one standard deviation of 9 samples. Dashed lines indicate model fit to experimental data. Average initial concentrations of Fe(II) and H_2O_2 were 4.59 and 5.56 μM, respectively. The yield of hTA is estimated to be 31.5 ±7%.

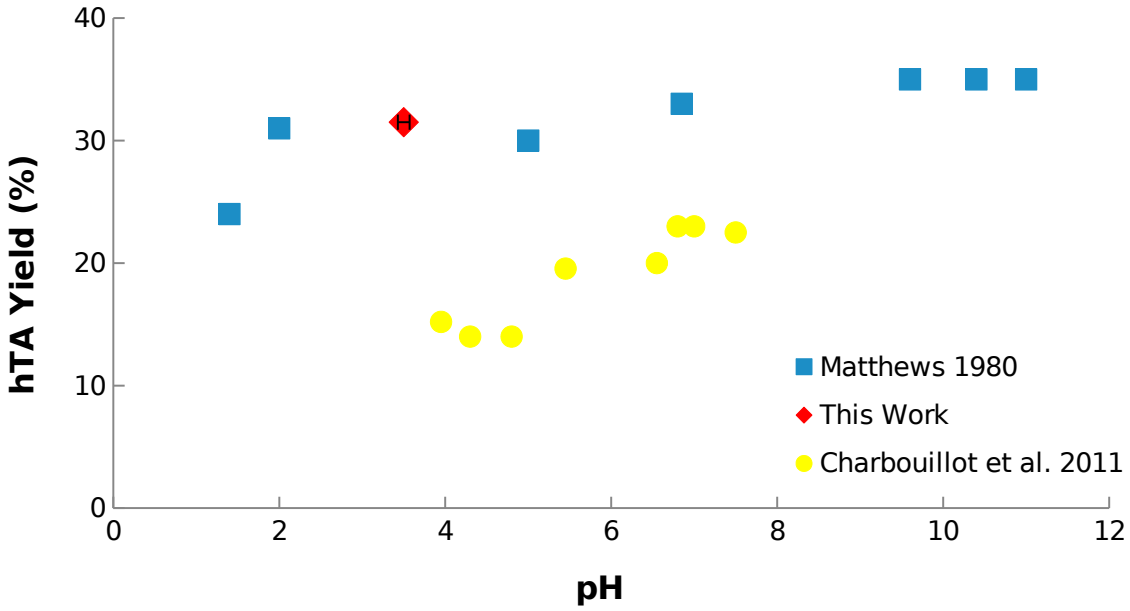

Figure 2. hTA yields as a function of pH. Matthews (1980) did not indicate error bars or the experimental temperature; Charbouillot et al. (2011) measurements were performed at 288 K; this work was performed at 293 K. Two other groups (Mark et al. 1998, Page et al. 2010) report values of 35% at unspecified pH.

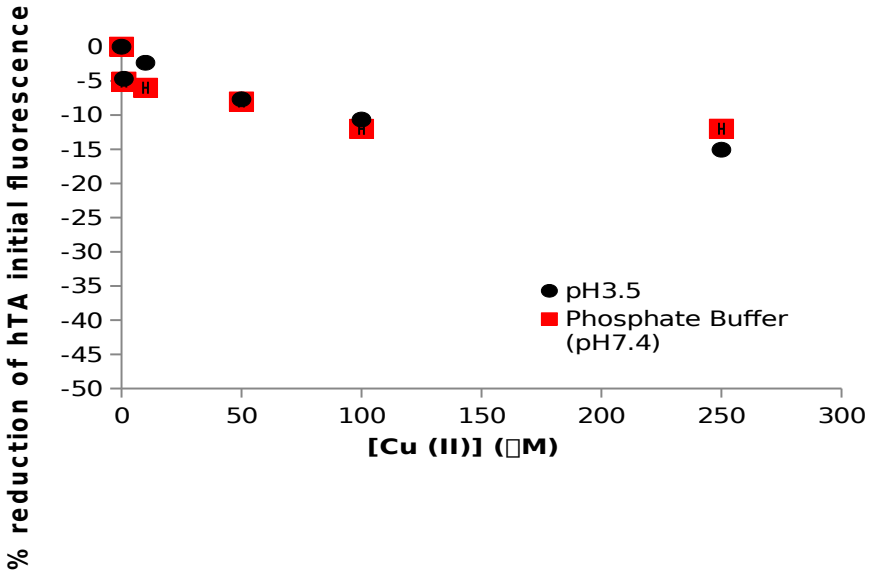

Figure 3. Reduction of hTA fluorescence intensity (at Ex/Em of 310/418 nm) by Cu(II).